Stellar archeology: a cosmological view of dSphs

Stefania Salvadori

Abstract The origin of dwarf spheroidal galaxies (dSphs) is investigated in a global cosmological context by simultaneously following the evolution of the Galaxy and its dwarf satellites. This approach enable to study the formation of dSphs in their proper birth environment and to reconstruct their own merging histories. The proposed picture simultaneously accounts for several dSph and Milky Way properties, including the Metallicity Distribution Functions of metal-poor stars. The observed features are interpreted in terms of physical processes acting at high redshifts.

1 Cosmological background

Today living metal-poor stars represent the fossil records of the early cosmic star formation. Indeed they are expected to form at high redshifts, as soon as the metal (and dust) content of the gas was high enough $Z > Z_{cr} = 10^{-4\pm1} Z_{\odot}$ [16] to trigger the formation of low-mass stars, which can survive until the present days. Extremely metal-poor stars ([Fe/H]< -3) have been observed in the Milky Way (MW) halo since long time ago [12]. However, the most promising objects to host these elusive stellar population are expected to be dwarf spheroidal galaxies (dSphs) that are metal-poor and old stellar systems, *all* of them showing the presence of a stellar population > 10 Gyr old, despite of very different star formation histories.

Recently, extremely metal-poor stars have been observed in nearby dSph galaxies [20]. However, while [Fe/H]< -3 stars represents the 25% of the total stellar mass in ultra-faint dwarfs (UFs, $L < 10^5 L_{\odot}$), they are extremely rare in the more luminous "classical" dSph galaxies ($\leq 6\%$ [19]). How did ultra-faint and classical dSphs form? More recently, high-resolution spectroscopic studies [4, 5, 9, 11, 20] have shown that, despite of this difference in number, the abundance patterns of

Stefania Salvadori
Kapteyn Astronomical Institute, Landleven 12, 9747 AD Groningen (NL)
e-mail: salvadori@astro.rug.nl

[Fe/H]< -3 stars is mainly consistent in these two class of galaxies. Hence, what is the origin of extremely metal-poor stars?

In this contribution I will present a possible *cosmological scenario* for the origin of dSphs, by investigating the formation of these galaxies along the build-up of the Milky Way. Other than simultaneously accounting for several dSphs and MW properties, the model will allow us to physically explain the above mentioned features pertaining to extremely metal-poor stars.

2 Star formation & feedback processes at high redshifts

The most relevant properties of the model can be summarized in few points (for an exhaustive description see [13] and [15]). A statistical significant sample of possible MW hierarchical merger histories is first reconstructed by using a Monte Carlo algorithm [13] based on the Extended Press & Schecter theory [1]. Hence, the evolution of gas and stars is followed along the hierarchical trees by assuming that in each halo the star formation (SF) rate is proportional to the mass of cold gas, whose gradual accretion is regulated by a numerically calibrated infall rate [14].

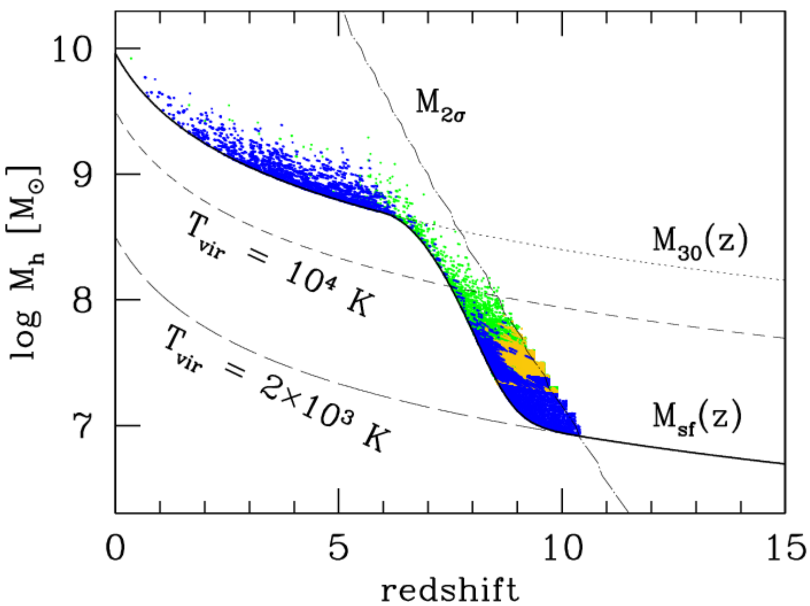

Fig. 1 Hosting halo mass and circular velocity of dSph candidates (points) in 10 possible MW merger histories as a function of the formation redshift. The gray scaling indicates the baryonic fraction f_b at the formation epoch with respect to the cosmic value $f_c = 0.156$: $f_b/f_c > 0.5$ (dark), $0.1 < f_b/f_c < 0.5$ (intermediate), $f_b/f_c < 0.1$ (light). The color version is available in [15]. The lines in the panel show the evolution of $M_{sf}(z)$ (solid), the halo mass corresponding to 2σ peaks (dotted-long dashed), $T_{vir} = 10^4$K (short dashed line) and $T_{vir} = 2 \times 10^3$K (long dashed line).

Additional hypothesis are required in order to include the effects of *radiative feedback* at high redshifts, influencing both the minimum halo mass required to form stars, $M_{sf}(z)$, and the SF efficiency of the star forming objects. Indeed the gradual reionization of the MW environment, completed by z_{rei}, suppress the SF in progressively more massive haloes. The evolution of $M_{sf}(z)$ adopted here (Fig.1) accounts for this effect, and assume $z_{rei}=6$. On the other hand, UV photons in the Lyman-Werner band can easily photodissociate H_2 molecules, which represent the only cooling agents of $T_{vir}<10^4$ K "minihaloes". We then assume that the SF efficiency of these objects is reduced by a factor $[1+(T_{vir}/2\times10^4\mathrm{K})^{-3}]^{-1}$ with respect to more massive H-cooling haloes [15].
By including the effects of *mechanical feedback* driven by supernovae (SN) energy deposition (we only include the effect of SN type II [14]), we follow self-consistently the chemical evolution of the gas in both the proto-galaxies and in the MW environment (Fig.2) i.e. the medium out of which the haloes virialize and accrete gas. The SF and the SN wind efficiencies are calibrated to *simultaneously* reproduce [13] the global properties of the MW (stellar/gas mass and metallicity) and the Metallicity Distribution Function of Galactic halo stars [17].

3 The birth environment

DSph candidates are selected among the star forming haloes ($M>M_{sf}(z)$) which are likely to become satellites i.e. those corresponding to density fluctuations $<2\sigma$ [3]. Their total dark matter mass, formation redshift and initial baryonic fraction (f_b) with respect to the cosmic value $f_c=\Omega_b/\Omega_m=0.156$, are shown in Fig. 1 (see [15] for more details). Note that, according to this picture, the hosting haloes of dSph galaxies are expected to form when $z<10.5$. In Fig. 2 the metallicity evolution of the MW environment is shown. We can note that the scatter is very big at high redshifts, reflecting the dispersion among different hierarchical merger histories and that the *average* iron-abundance rapidly increases at decreasing redshifts reaching [Fe/H]≈ -4 when $z=15$. This implies that *the MW satellites form out of a birth environment that is naturally pre-enriched* due to SN explosions along the build-up of the Galaxy [14].

4 Mass and formation epochs

In Fig. 3 the observed and simulated Iron-Luminosity relations are compared. The faint end of the relation, $L<10^6L_\odot$, is predominantly populated by $T_{vir}<10^4$ K minihaloes, in which the SF is strongly reduced due to ineffective molecular hydrogen cooling (Sec. 2). Above that luminosity H-cooling haloes dominates. We then infer that *ultra-faint dSphs are the living fossils of star forming minihaloes*. As these objects virialize when $z>7.5$ and have total masses $M\approx10^{7-8}M_\odot$ (Fig. 1),

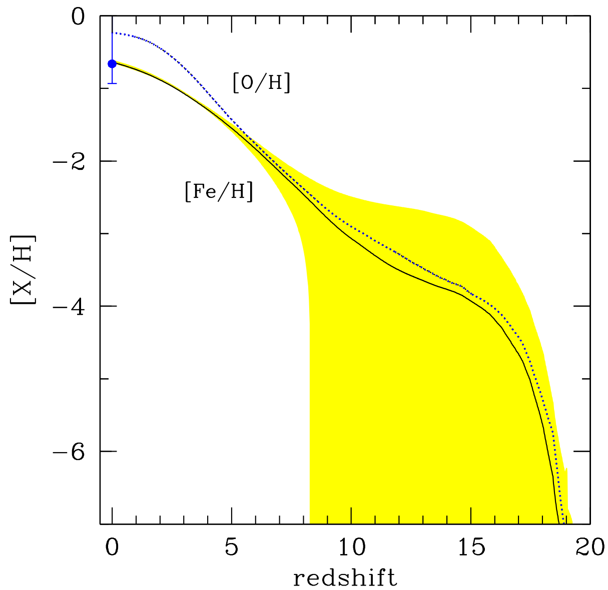

Fig. 2 Evolution of the iron (solid line) and oxygen (dotted line) abundance in the Galactic environment. Lines are the average values over 100 possible MW hierarchical merging histories. The shaded area delimits the $\pm 1\sigma$ dispersion region for [Fe/H]. The point is the measured [O/H] in high velocity clouds [6].

we conclude that *ultra-faint dwarfs are the oldest and the more dark matter dominated ($M/L > 100$) dSphs in the MW system* [15]. On the contrary, classical dSph galaxies are associated to more massive H-cooling haloes, which more efficiently cool down their gas and assembled at later times. Sculptor-like dSphs, for example, have total masses $M \approx 10^{8.5} M_{\odot}$, and finally form when $z = 6.5$. Can we find the imprints of such a different origin in the observed properties of dSphs?

5 Metallicity Distribution Functions

Let's compare the average MDF of ultra-faint and Sculptor-like candidates with the observational data (Fig. 4). The agreement is quite good, thus allowing us to interpret the different MDF shapes in terms of physical mechanisms. According to our results the width of the MDFs reflects the cooling-efficiency of the gas: ultra-faint dwarfs have a broader distribution because of the extremely low SF rate ($< 0.01 M_{\odot}$/yr) caused by ineffective H_2-cooling. Few supernovae explode in these galaxies, which therefore slowly enrich and eject their gas. Sculptor-like dSphs, instead, reach high SF values ($> 0.1 M_{\odot}/$ yr) at their final assembling epoch, thus experiencing a rapid metal enrichment along with a strong gas ejection [14]. The

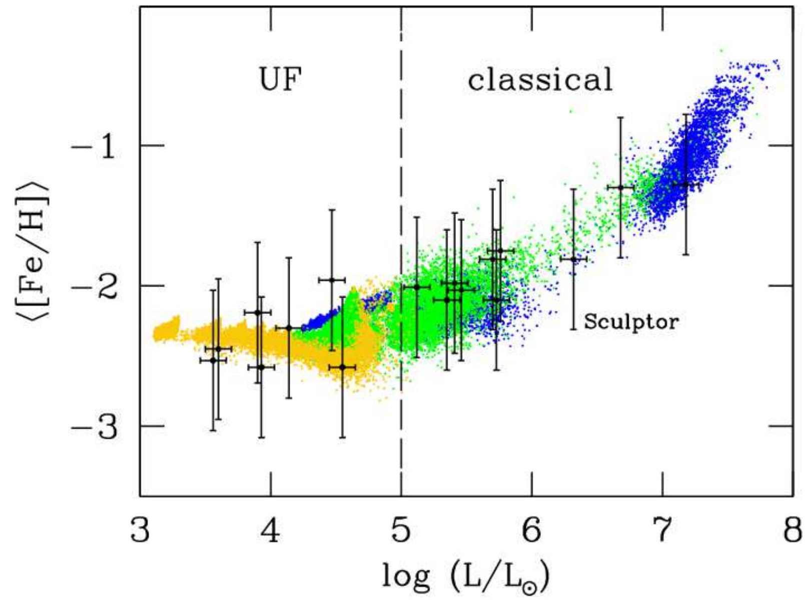

Fig. 3 Total luminosity of the dSph candidates selected in 10 possible MW merger histories as a function of their average iron-abundance (colored points). The gray scaling shows the baryonic fraction f_b at the formation epoch with respect to the cosmic value as in Fig. 1 (the color version is available in [15]). Points with error bars are the observational data collected by [8].

pronounced peak of the MDF and the prompt decrease for [Fe/H]> -1.5 reflect these features [14].
On the other hand, the shift of the ultra-faint MDF towards lower [Fe/H] values is a result of the lower metallicity of the MW environment at their higher formation epochs. Indeed UFs form at $z > 8.5$ when *pre-enrichment* of the MW environment was [Fe/H]< -3.5 while Sculptor-like dSphs finally assembled at later times, when [Fe/H]≈ -3 [14]. Note however that the model predicts a small [Fe/H]< -3 tail in the Sculptor MDF [15] that now has been confirmed by the new results of the DART team [19]. What is then the origin of these extremely metal-poor stars?

6 Merging and star formation histories

We can answer to this question by analyzing the star formation history of a typical Sculptor-like dSph (Fig. 5) which exhibits several bursts of different intensity and duration. The highest peak corresponds to the SF activity at the final assembling epoch ($z \approx 6.5$). Mechanical feedback is so efficient at that time (because of the high SF rate) that the galaxy blow out the entire gas reservoir in few hundred of Myr, thus suddenly stopping the SF. Fresh gas returned by evolved stars is grad-

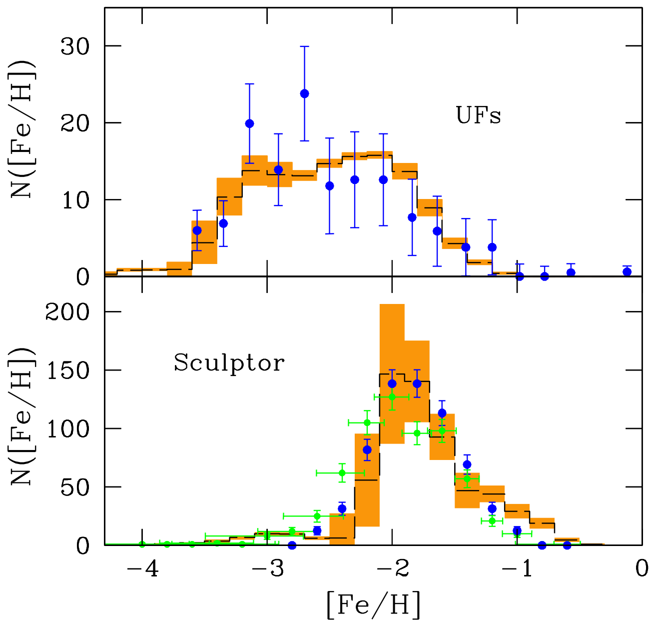

Fig. 4 Observed (points) and simulated (histogram) MDF of UFs (*top*) and Sculptor dSph (*bottom*). Histograms are the averaged MDF over all UFs ($L < 10^5 L_\odot$ *top*) and Sculptor ($10^6 L_\odot < L < 10^{6.5} L_\odot$ *bottom*) candidates in 10 merger histories. The shaded area is the $\pm 1\sigma$ scatter among different realizations. The data points are by [8] (*top*, Poissonian errors) and by the DART team (*bottom*) using the old (darkest points, Poissonian errors [7]) and the new (lightest points, observational errors [19]) CaT line calibration.

ually collected after this event, and the SF re-start again until a new blow away occurs [14]. However the rates are extremely low ($SF < 0.0005 M_\odot$/yr) because of the paucity of returned gas, and only a few percent of the total stellar mass is formed during this phase. At earlier times ($t - t_{form} < 0.5$ Gyr) instead, the peaks reflect the star formation and merging activity of the Sculptor progenitor haloes. We find that the oldest progenitors are *minihaloes* that form stars at very high redshifts $z > 9$ and with typical SF rates $< 0.02 M_\odot$/yr. The extremely metal-poor stars that populate the lowest metallicity tail of the Sculptor MDF formed in these objects, and hence have *the same origin of those found in ultra-faint galaxies.*

7 Conclusions

Stellar archeology of the most metal-poor stars may provide fundamental insights on the early cosmic star formation. In particular the properties of the observed Metal-

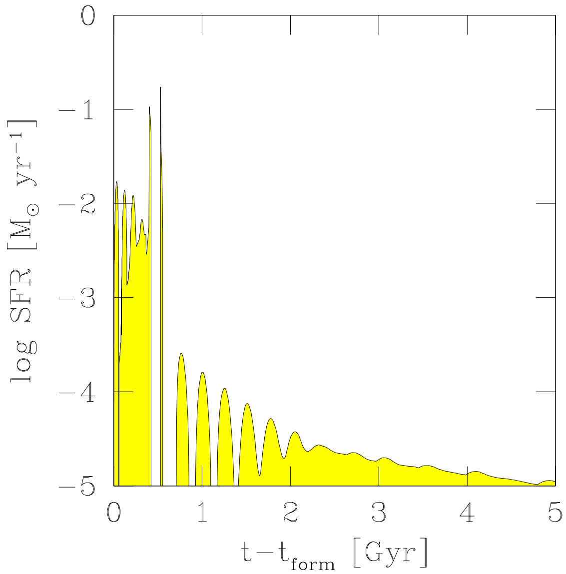

Fig. 5 Star formation history of a typical Sculptor-like dSph galaxy.

licity Distribution Functions in nearby dSph galaxies can be used to constrain the origin of these Galactic satellites and to study the physical processes occurring at high redshifts. Ultra Faint dSphs are expected to be the today-living counterpart of high redshift H_2-cooling minihaloes ($M = 10^{7-8} M_{\odot}$) which are very ineffectively SF objects turning into stars $< 3\%$ of the potentially available cosmic baryons [15]. This result is consistent with recent *complementary studies* [2, 10] that use simulations to investigate the origin of dSphs and account for the luminosity function of the MW satellites.

According to our picture the higher fraction of [Fe/H]< -3 stars in ultra-faint with respect to classical dSphs reflects both the lower SF rate, caused by ineffective H_2 cooling, both the lower metal (pre-)enrichment of the MW-environment at their further formation epoch. Classical dSphs, indeed, are expected to be associated with massive H-cooling haloes ($M > 10^8 M_{\odot}$) that more efficiently cool-down their gas and that form at later times ($z < 7.5$) through merging of many progenitor haloes. Although extremely rare [Fe/H]< -3 stars are expected to populate *all* classical dSphs. Indeed these stars are expected to mainly form at high redshifts in H_2-cooling minihaloes, that at later times naturally assemble in more massive dSphs. These findings can explain both the detection of [Fe/H]< -3 stars in nearby classical dSphs [20] and the existence of an old stellar population in *all* of them [21].

References

1. J. R. Bond et al. : ”Excursion set mass functions for hierarchical Gaussian fluctuations” *ApJ*, **379**, 440–460 (1991)
2. M. Bovill & M. Ricotti : ”Pre-Reionization Fossils, Ultra-Faint Dwarfs, and the Missing Galactic Satellite Problem” *ApJ*, **693**, 1859–1870 (2009)
3. J. Diemand, P. Madau, B. Moore : ”The distribution and kinematics of early high- peaks in present-day haloes: implications for rare objects and old stellar populations” *MNRAS*, **364**, 367–383 (2005)
4. A. Frebel, E. N. Kirby & J. D. Simon : ”Linking dwarf galaxies to halo building blocks with the most metal-poor star in Sculptor” *Nature*, **464**, 72–75 (2010)
5. A. Frebel, J. D. Simon, M. Geha & B. Willman : ”High-Resolution Spectroscopy of Extremely Metal-Poor Stars in the Least Evolved Galaxies: Ursa Major II and Coma Berenices” *ApJ*, **708**, 560 (2010)
6. D. Ganguly, K. R. Sembach, T. M. Todd, B. D. Savage : ”Highly Ionized Gas in the Galactic Halo and the High-Velocity Clouds toward PG 1116+215” *ApJ*, **157**, 251–278 (2005)
7. A. Helmi et al. : ”A New View of the Dwarf Spheroidal Satellites of the Milky Way from VLT FLAMES: Where Are the Very Metal-poor Stars?” *ApJ*, **651**, L121-L124 (2006)
8. E. N. Kirby, J. D. Simon, M. Geha, P. Guhathakurta. & A. Frebel : ”Uncovering Extremely Metal-Poor Stars in the Milky Way’s Ultrafaint Dwarf Spheroidal Satellite Galaxies” *ApJ*, **685**, L43–L46 (2008)
9. A. Koch et al. : ”A Spectroscopic Confirmation of the Bootes II Dwarf Spheroidal” *ApJ*, **690**, 453–462 (2009)
10. J. A. Mũnoz, P. Madau, A. Loeb & J. Diemand : ”Probing the epoch of reionization with Milky Way satellites” *MNRAS*, **400**, 1593–1602 (2009)
11. J.E. Norris et al. : ”Chemical Enrichment in the Faintest Galaxies: The Carbon and Iron Abundance Spreads in the Botes I Dwarf Spheroidal Galaxy and the Segue 1 System” *ApJ*, **723**, 1632–1650 (2010)
12. S. G. Ryan & J. E. Norris : ”Subdwarf Studies. III. The Halo Metallicity Distribution” *AJ*, **101**, 1865–1878 (1991)
13. S. Salvadori, R. Schneider & A. Ferrara: ”Cosmic stellar relics in the Galactic halo” *MNRAS* **381**, 647–662 (2007)
14. S. Salvadori, A. Ferrara & R. Schneider: ”Life and times of dwarf spheroidal galaxies” *MNRAS* **386**, 348–358 (2008)
15. S. Salvadori & A. Ferrara: ”Ultra faint dwarfs: probing early cosmic star formation” *MNRAS* **395**, L6–L10 (2009)
16. R. Schneider et al. : ”Low-mass relics of early star formation” *Nature*, **422**, 869–871 (2003)
17. T. Schoerck et al.: ”The stellar content of the Hamburg/ESO survey. V. The metallicity distribution function of the Galactic halo” *A&A*, **507**, 817–832 (2009)
18. J. D. Simon et al.: ”High-resolution Spectroscopy of Extremely Metal-poor Stars in the Least Evolved Galaxies: Leo IV” *ApJ*, **716**, 446–452 (2010)
19. E. Starkenburg et al. : ”The NIR Ca ii triplet at low metallicity. Searching for extremely low-metallicity stars in classical dwarf galaxies” *A&A*, **513**, idA34 (2010)
20. M. Tefelmeyer et al.: ”Extremely metal-poor stars in classical dwarf spheroidal galaxies: Fornax, Sculptor, and Sextans” *A&A*, **524**, idA58 (2010)
21. E. Tolstoy, V. Hill & M. Tosi : ”Star-Formation Histories, Abundances, and Kinematics of Dwarf Galaxies in the Local Group” *ARA&A*, **47**, 371–425 (2009)